J. Fluid Mech. (1973), *vol.* 57, *part* 2, *pp.* 257–268
Printed in Great Britain

Acoustically driven water waves

By R. E. FRANKLIN, M. PRICE AND D. C. WILLIAMS
Engineering Laboratory, University of Oxford

(Received 28 July 1972)

If the air in a resonance tube half-filled with water is driven at an acoustic resonant frequency, surface waves of much lower frequency may also be excited. Experiments on this phenomenon are reported and compared with the theory of spatial resonance.

1. Introduction

Some time ago, one of us (Franklin 1969, unpublished) carried out in simple form an experiment suggested by J. Ockenden (1969, private communication). In this experiment a horizontal glass tube about 1·5 m long, 0·05 m in diameter and closed at both ends was half-filled with water and then driven as an acoustic resonance tube. A curious effect was observed in that as the driving frequency approached certain resonant frequencies of the air, standing waves of different wavenumber and very different frequency were set into motion in the water surface.

The results of this experiment, together with observations of a similar and probably related phenomenon made by Huntley (1972) when mechanically vibrating open-topped cylinders containing water, have been considered by Mahony & Smith (1972), who have suggested an explanation. In essence, their argument runs as follows,

If the air is driven at a circular frequency ω near the natural frequency of an acoustic mode of wavenumber k, and the water surface oscillates at a frequency σ in a mode of wavenumber κ, then the acoustic field basically contains two components of the form $\cos\omega t\cos kx$ and $\cos\sigma t\cos\kappa x$, where the x co-ordinate is measured down the tube.

In arriving at this statement the kinematic condition at the air–water interface is taken to be

$$\Phi_z = \zeta_t \quad \text{on} \quad z = 0,$$

where Φ is the velocity potential of the acoustic field, ζ the elevation of the water surface above the horizontal plane $z = 0$ and the suffixes z and t denote differentiation with respect to the z co-ordinate and time. If, however, second-order terms are included, this condition becomes

$$\Phi_z + \Phi_{zz}\zeta = \zeta_t + \Phi_x\zeta_x \quad \text{on} \quad z = 0,$$

and since the water surface has the form $\cos\sigma t\cos\kappa x$, the second-order terms can generate expressions of the form

$$(\cos\omega t\cos kx + \cos\sigma t\cos\kappa x)\cos\sigma t\cos\kappa x,$$

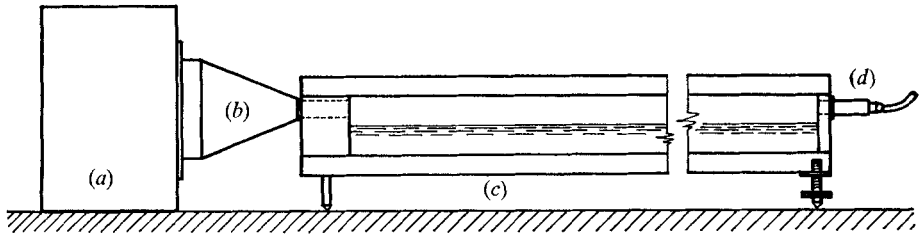

FIGURE 1. Diagram of apparatus. (*a*) Loudspeaker driving unit. (*b*) Conical coupler. (*c*) Resonance tube. (*d*) Microphone.

the first factor of which may be put into the form

$$(\cos(\omega+\sigma)t+\cos(\omega-\sigma)t)(\cos(\kappa+k)x+\cos(\kappa-k)x).$$

From this one concludes that, if $\kappa-k=k$ and σ is small enough for the frequencies $\omega+\sigma$ and $\omega-\sigma$ still to lie within the resonant bandwidth of the mode, the acoustic field is likely to contain further appreciable components of the form

$$\cos(\omega\pm\sigma)\cos kx.$$

A second boundary condition must be applied at the interface, namely Bernoulli's equation, from which the surface pressure is calculated. If this boundary condition is also evaluated to second order, it contains the squares of the acoustic velocities, and the components of the acoustic field having the forms $\cos kx\cos\omega t$ and $\cos kx\cos(\omega\pm\sigma)t$ can give rise to expressions of the form

$$\cos^2 kx(\cos\omega t+\cos(\omega\pm\sigma)t)^2,$$

which, when expanded, is found to contain a component

$$\tfrac{1}{2}\cos 2kx\cos\sigma t=\tfrac{1}{2}\cos\kappa x\cos\sigma t.$$

There are, therefore, components in the pressure field which can drive the water waves and the possibility of a sustained motion exists.

The observations on the simple rig confirmed the broad outline of this argument and the phenomenon therefore seemed to merit detailed investigation. In this report we describe experiments carried out on a rather more sophisticated rig and we compare our results quantitatively with the theory.

2. Apparatus

The apparatus, which is shown diagrammatically in figure 1, consists basically of a closed resonance tube of length 1·435 m having a rectangular cross-section 0·051 m wide and 0·076 m deep. Two lengths of aluminium channel form the top and bottom of the tube, the sides are of perspex sheet and the ends are closed with aluminium blocks in which holes have been drilled to take at one end a $\frac{1}{2}$ in. diameter Bruel & Kjaer condenser microphone, and at the other the outlet tube from the loudspeaker driving unit.

The driving loudspeaker, which has a diaphragm of diameter 0·08 m, is mounted inside a box and coupled to the resonance tube by a simple conical coupler terminating in a tube with an internal diameter of 0·01 m. In early experiments, the loudspeaker was driven by a Ling Dynamic Systems TPO 20

oscillator, but as the work proceeded it became clear that the accuracy to which it was necessary to work was such that the drift in this instrument was unacceptable. Accordingly, a Muirhead–Wigan decade oscillator type D980A was subsequently used as a stabilized source for the TPO 20, which then was used merely as a power amplifier. This question of accuracy arose again in the determination of the frequency of the driving signal. In the frequency range of the experiment it proved more accurate to measure the period of the signal with a Hewlett–Packard electronic counter and to obtain the frequency by inversion.

As implied above, the acoustic field in the tube was detected using a $\frac{1}{2}$ in. diameter Bruel & Kjaer condenser microphone, flush-mounted in the end-block. The signal from the microphone was amplified through a Bruel & Kjaer spectrometer type 2112.

The depth variation of the water was measured by constructing a simple photo-electric transducer. In this transducer, a beam of light from a 100 W bulb is modulated by the water (made opaque by adding Duckhams Aquicut 40 soluble oil) and then falls on one of two Ferranti MS2BE photo-voltaic cells, the second of which acts as a reference and is wired in series with the first such that their voltages subtract. The transducer is mounted on the channel and may be moved to a position opposite an antinode; the cells may also be moved vertically within the transducer mounting, thus enabling readings to be taken at several fluid depths. The output of the transducer was fed to a pen-recorder, and the system calibrated against a travelling microscope.

3. Theoretical results

According to Mahony & Smith (1972), the appearance of the low-frequency standing waves in the water surface is a consequence of an instability in the set of equations they derive to describe the system. Regions of stability and instability may be defined in the plane of B, the amplitude of the acoustic drive, and Δ, the difference between the driving frequency and the resonant frequency of the acoustic mode. These regions are separated by the marginal-stability curves.

The amplitude of the acoustic response is shown to be given by

$$|\Phi_0| = B/(\nu^2+\Delta^2)^{\frac{1}{2}}, \tag{3.1}$$

where ν is the logarithmic decay rate of the acoustic mode, and in terms of this parameter rather than B, the marginal-stability curves are given by

$$|\Phi_0|^2 = \begin{cases} -\frac{1}{2}\sigma(\nu^2+\Delta^2)/\alpha\beta\Delta & \text{for} \quad \Delta < 0, \qquad (3.2) \\ \frac{1}{4}\dfrac{\nu'}{\nu}\dfrac{\{(\Delta^2+\nu^2-\sigma^2)^2+4\nu^2\sigma^2\}}{\alpha\beta\Delta\sigma} & \text{for} \quad \Delta > 0, \qquad (3.3) \end{cases}$$

in which ν' is the logarithmic decay rate of the standing water waves and α and β are real constants.

Mahony & Smith also give equations from which $|\eta|$, the amplitude of the water waves, may be calculated. Thus, by elimination between equations (18) and (20) of their paper one finds that

$$\alpha^2\eta\eta^* = \tfrac{1}{2}(\Delta^2-\sigma^2-\nu^2) \pm [|\Phi_0|^2\alpha\beta\Delta\nu/\nu' - \nu^2\Delta^2]^{\frac{1}{2}}. \tag{3.4}$$

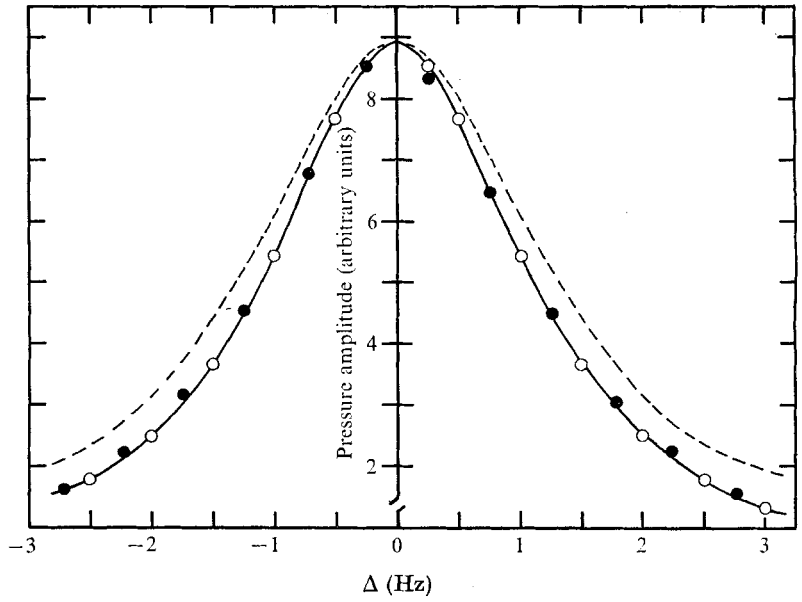

FIGURE 2. Measurements of acoustic damping. ●, resonance test data; ○, best fit to data, $\nu = 1{\cdot}25\,\mathrm{s}^{-1}$; – – –, curve using measured decay rate of $\nu = 1{\cdot}00\,\mathrm{s}^{-1}$.

4. Experimental procedure and results

4.1. *Measurement of basic parameters*

The acoustic resonant frequencies. The acoustic resonant frequencies were determined by measuring the frequencies at which the microphone output rose to a maximum as the driving frequency was changed at constant power input. Two sets of maxima were found, one of which corresponded to the tube resonances and the other (subsequently ignored) to resonances of the complete loudspeaker-coupler-tube system.

Initial experiments had shown that the water waves were excited over only narrow ranges of frequency, and it proved necessary to measure the resonant frequencies to within $\pm 0{\cdot}005$ Hz. At this accuracy, the effects of temperature changes are appreciable and so throughout the experiments the appropriate resonance was determined for each run and the results compared by introducing the proper corrections.

The damping of the acoustic wave. Damping measurements were carried out in two ways: first by measuring the decay rate directly and second by plotting a frequency–response curve.

To measure the decay rate, the output from the Bruel & Kjaer spectrometer was displayed on a Tektronix storage oscilloscope type 564. A sweep was triggered just before the power input to the loudspeaker was interrupted, and the resulting trace analysed.

In the second method, the variation in the acoustic wave amplitude was measured as a function of frequency at constant input power. Equation (3.1) was then fitted to the results by matching the maximum values of $|\Phi_0|^2$ and choosing the value of ν that gave the best fit. A typical set of results is given in figure 2.

(*a*) Decay rate measurements		(*b*) Frequency response measurements	
Frequency (Hz)	ν (s^{-1})	Frequency (Hz)	ν (s^{-1})
364·60	1·39	363·86	1·67
247·60	1·36	243·00	1·36
136·20	1·49	126·73	1·25

TABLE 1. Measurements of acoustic damping

Acoustic frequency (Hz)	Water-wave frequency (Hz)	ν' (s^{-1})
125·33	0·445	0·0091
240·80	0·857	0·0137
366·80	1·200	0·0236

TABLE 2. Measurements of water-wave damping

In all cases, the values of decay rate found by the two methods agree within the limits of experimental accuracy: this may be seen by comparing the results of tables 1 (*a*) and (*b*). Since the second method gives slightly better accuracy, the values of table 1 (*b*) have been used in all calculations.

The water-wave resonant frequencies. The resonant characteristics of the water-wave system were investigated in two ways. In the first, the resonance tube was oscillated in the direction of its length by placing it on a trolley driven from an eccentric cam mounted on the spindle of an infinitely variable speed gearbox. For several modes, the driving frequency was adjusted until the amplitude of the standing-wave system reached a maximum, and the frequency then measured both by counting against a stop-watch and from pen-recorder traces of the surface-displacement transducer.

This method does not excite all the modes of the system: in particular it does not excite those at which the interaction between the acoustic field and the water wave occurs. Thus the second method employed was that of acoustic excitation. Again the acoustic driving frequency was adjusted until the amplitude of response of the water wave reached a maximum in each of a series of modes, and the water-wave resonant frequencies measured. The results from the two methods agreed well.

The damping of the water waves. The logarithmic decay rate of the standing water waves was measured from traces taken with a pen-recorder of the output of the surface-displacement transducer after the drive was interrupted. For these measurements the acoustic drive was used, for it was difficult to stop the mechanical drive without introducing a travelling wave disturbance. Typical results are given in table 2.

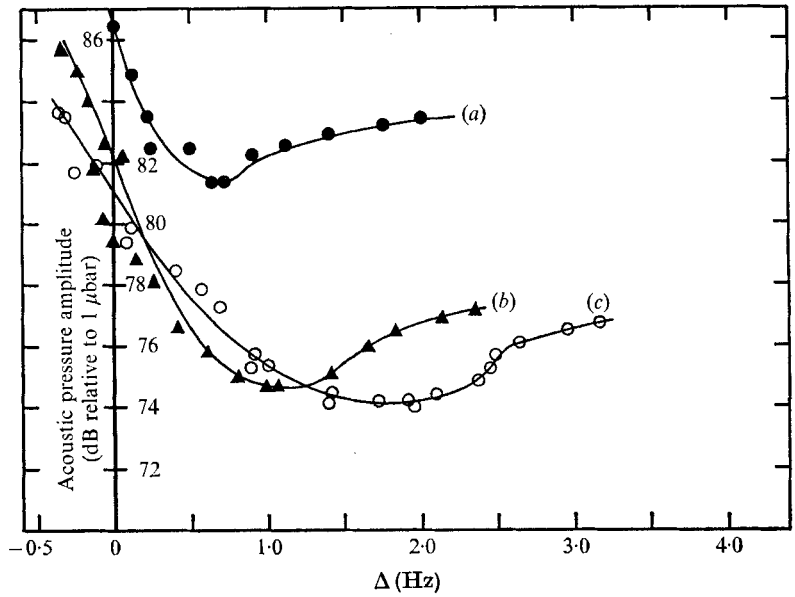

FIGURE 3 Marginal-stability curves. (*a*) Nominal resonance 126 Hz. (*b*) Nominal resonance 247 Hz. (*c*) Nominal resonance 363 Hz.

4.2. *Curves of marginal stability*

The curves of marginal stability were determined for a given acoustic mode by measuring, at selected values of the frequency difference Δ, the amplitude of the acoustic pressure at which the presence of standing water waves was first detected. Since the microphone is more sensitive in this respect than the surface-displacement transducer, the technique was to increase slowly the input power until the first stable modulation of the acoustic pressure was observed. The acoustic pressure was then measured in decibels relative to an arbitrary level.

During the course of the experiments it quickly became clear that the instability could be triggered prematurely if the input power was suddenly increased. Further, if the modulation became large, the input power had to be reduced to allow the motion to die away, for once it was set in motion, the surface wave could be maintained with a lower power than that required to start it.

Temperature changes had a considerable effect on Δ through the consequent changes in the resonant frequency. Two methods were available for correcting Δ. The first was a simple calculation of the corrected resonant frequency, but although this was adequate when the light source of the displacement transducer was off, it was difficult to apply when the light source was on, for the temperature inside the tube was then different from room temperature and probably of non-uniform distribution. In these cases the second method was used: the acoustic resonant frequency and temperature were measured before and after a given set of readings and a linear interpolation made.

The results for the three acoustic modes with nominal resonant frequencies of 126, 247 and 363 Hz are shown in figure 3.

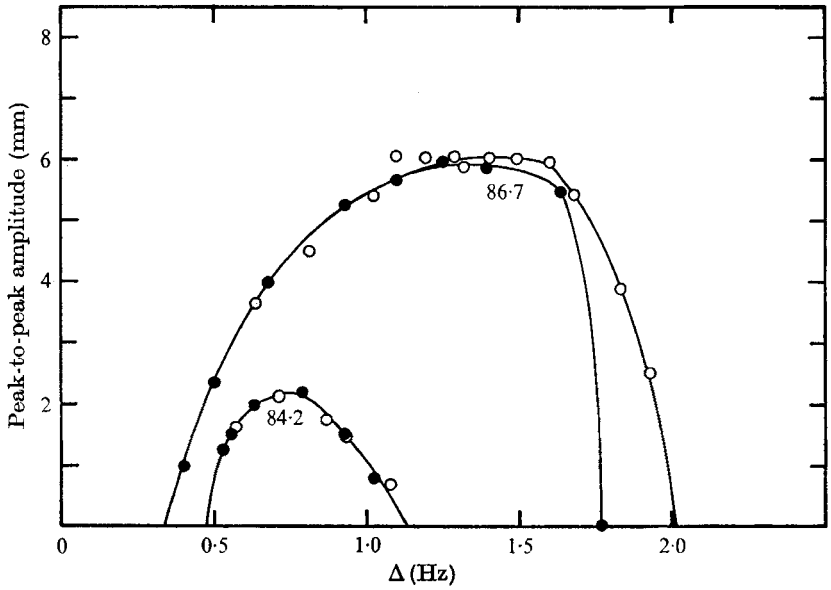

FIGURE 4. Water-wave amplitude. Nominal resonance 126 Hz. ○, frequency increasing; ●, frequency decreasing. Numbers against curves are acoustic pressures in dB relative to 1 μbar.

4.3. *Variation of water-wave amplitude with frequency*

The variation of the water-wave amplitude with frequency was measured for the three acoustic modes with nominal frequencies of 126, 247 and 363 Hz for a constant depth of about 0·0395 m and at least two different power settings.

For each run, the acoustic resonant frequency was first found and the input power then set to give a particular value of the acoustic pressure amplitude. With the input power held constant at this value, Δ was increased in steps by adjusting the driving frequency and for each value, after the transient motions had died away, a reading was taken from the surface-displacement transducer. Eventually a value of Δ was reached at which the surface-wave amplitude fell to zero; at this point a new determination of the resonant frequency was made and a linear temperature correction made to the results. Starting again from the value of Δ at which the surface-wave amplitude had fallen to zero, readings were now taken as Δ was decreased to a lower limit at which the surface-wave amplitude again fell to zero. If this lower limit of Δ lay below the resonant frequency, readings were taken until Δ was returned to zero. A final measurement of the resonant frequency was then made.

The results for the lowest frequency mode are shown in figure 4; data for the other two modes are introduced below.

5. Comparisons with theory

5.1. *Marginal-stability curves*

Using the experimentally determined values of ν, ν' and σ, equations (3.2) and (3.3) may be evaluated and the results plotted as a graph of $\alpha\beta|\Phi_0|^2$, in decibels

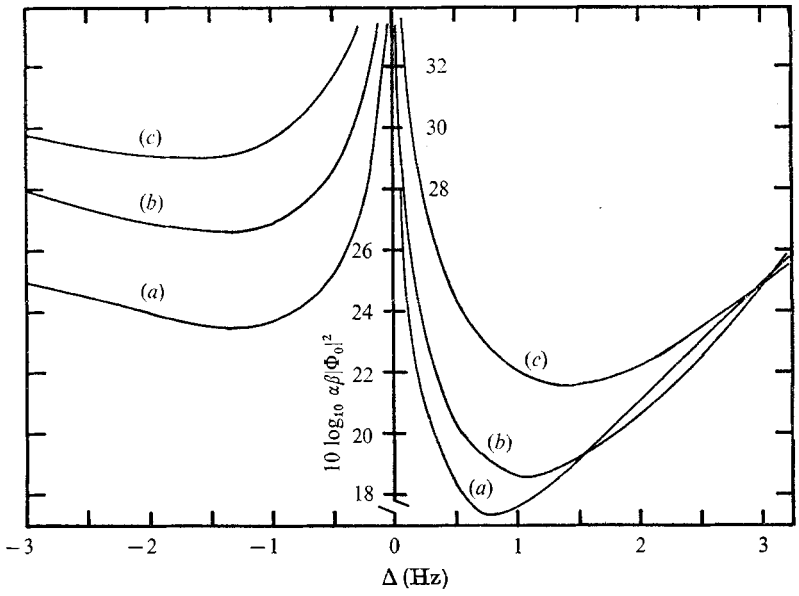

FIGURE 5. Theoretical marginal-stability curves. (*a*) Nominal resonance 126 Hz. (*b*) Nominal resonance 247 Hz. (*c*) Nominal resonance 363 Hz.

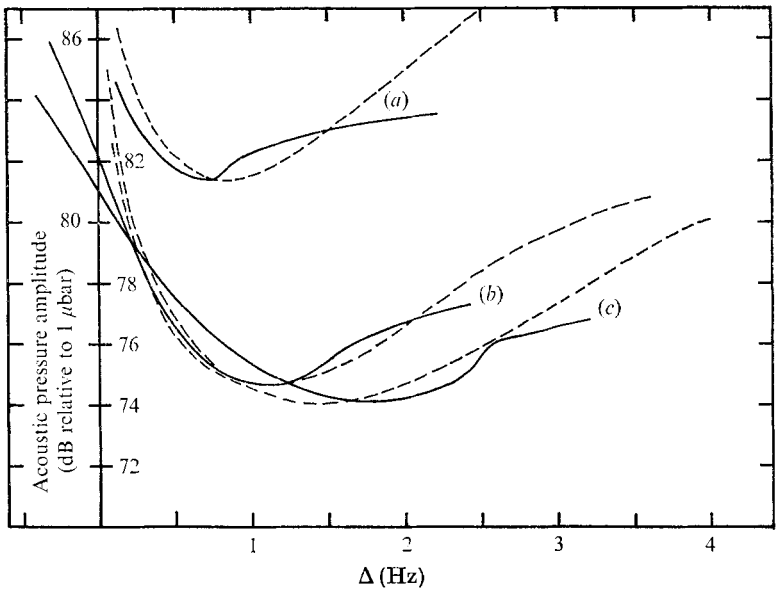

FIGURE 6. Marginal-stability curves. ——, experiments; – – –, theory. (*a*) Nominal resonance 126 Hz. (*b*) Nominal resonance 247 Hz. (*c*) Nominal resonance 363 Hz.

relative to an arbitrary level, as a function of Δ. This relationship is shown in figure 5 for the three modes for which data have been secured.

It is now a simple matter to apply a vertical shift to the theoretical curves in order to compare them with the experimental curves. The results are shown in figure 6, where the minima of the curves have been matched, and it is seen that

the theoretical and experimental curves have basically the same shape. Considerable differences appear in the region of $\Delta = 0$, but this is to be expected. It is possible that the experimental curves may join the two branches of the theoretical stability curves, but the data are insufficient to demonstrate the point.

5.2. *Variation of water-wave amplitude with frequency*

The experimental data are compared with equation (3.4) by choosing values of the constants α and β such that the maxima of the theoretical and experimental curves coincide. The value of $|\Phi_0|^2\alpha\beta$ which satisfies this condition may be shown (Price & Williams 1972) to be given by

$$|\Phi_0|^2\alpha\beta = \frac{2\Delta_m\nu'(\nu^2+\Delta_m^2)}{\sigma\nu(\nu^2-\Delta_m^2)^2}\{(\nu^4+\Delta_m^4) \pm [(\nu^4+\Delta_m^4)^2-\nu^2(\nu^4-\Delta_m^4)(\nu^2-\Delta_m^2)]^{\frac{1}{2}}\},$$

where Δ_m is the value of Δ at which $\eta\eta^*$ is found experimentally to be a maximum.

This value may be substituted into (3.4) together with Δ_m, and α^2 then chosen so that the theoretical and experimental maxima of $\eta\eta^*$ agree.

The results of all the experiments and the associated calculations are shown in figures 7 (*a*), (*b*) and (*c*), and it is seen that there is a general agreement between the theoretical and experimental curves. In detail, the agreement is good at low input powers but deteriorates at the higher inputs.

At the higher input powers an additional effect appears, for it becomes clear that there are two branches to the curves, one for increasing values of Δ, the other for decreasing values. The important difference between these two branches is that the curve for Δ increasing extends to greater values of Δ than that for which Δ is decreasing.

5.3. *Values of the constants α and β*

The amount by which the curves of figure 5 have to be shifted to correspond with the experimental data of figure 3 may be used to make an estimate of the value of $\alpha\beta$. Noting that the measured pressure is related to the velocity potential by the equation

$$|p| = \rho\omega|\Phi_0|,$$

it is a simple matter to show that

$$\begin{aligned} 10\log|\Phi_0|^2 &= 10\log(p^2_{\text{r.m.s.}}/p^2_{\text{ref}}) + 10\log p^2_{\text{ref}} + 10\log 2 - 10\log(\rho\times 2\pi f)^2 \\ &= SPL - 34{\cdot}7 + 20\log f, \end{aligned}$$

where SPL is the sound pressure level in decibels relative to $1\,\mu$bar, f is the frequency in Hz and the density of air has been taken to be $1{\cdot}22\,\text{kg/m}^3$. Comparison of this result with the calculated values of $10\log\alpha\beta|\Phi_0|^2$ gives estimates of $10\log\alpha\beta$.

The values of α and β and therefore that of $10\log\alpha\beta$ may be calculated from the formulae given by Mahony & Smith, and the theoretical values of this are compared with the experimental values in table 3. It is seen that the agreement is good at the lowest frequency. At the two higher frequencies the agreement is poorer, but one notes that the discrepancy is of the correct sign for, since the instability grows more slowly the smaller the amount by which the amplitude

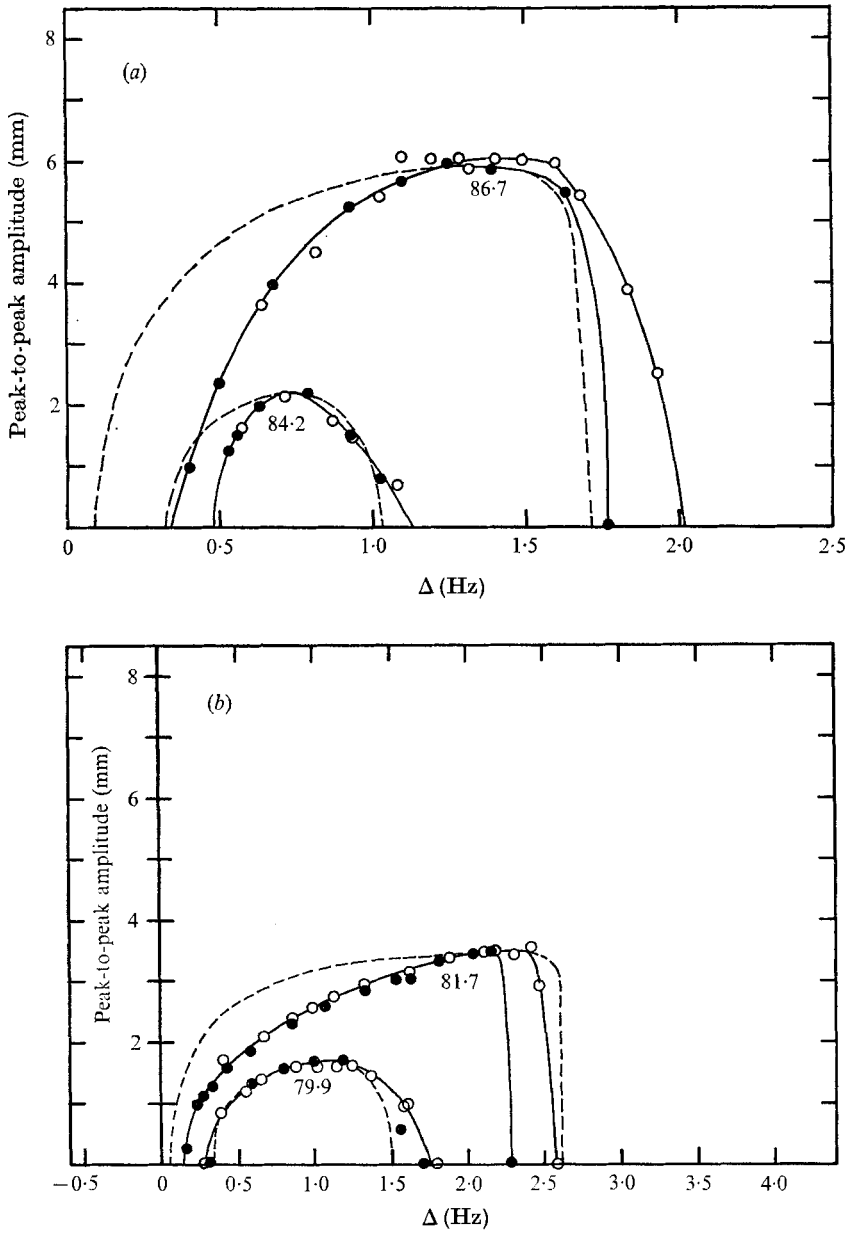

FIGURE 7. For legend see facing page.

of the drive exceeds that required at the margin of stability, one would expect the value of SPL to be too high.

The values of α obtained in the comparison of the theoretical and experimental results for the water-wave amplitude are not very accurate: they differ from the theoretical values by a factor lying between $\frac{1}{3}$ and $\frac{1}{4}$.

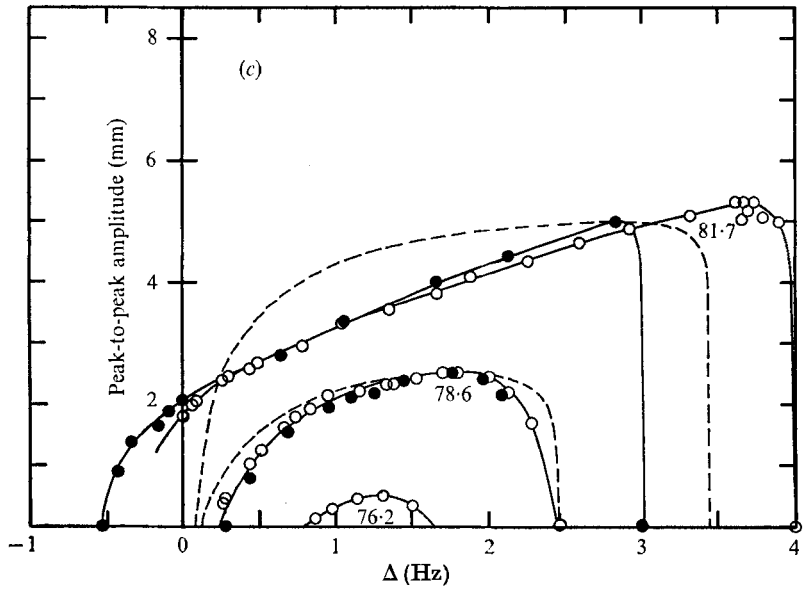

FIGURE 7. Water-wave amplitude. ○, experimental, frequency increasing; ●, experimental frequency decreasing; ---, theory. Numbers against curves are acoustic pressures in dB relative to 1 μbar. (*a*) Nominal resonance 126 Hz. (*b*) Nominal resonance 247 Hz. (*c*) Nominal resonance 363 Hz.

Nominal frequency (Hz)	$10\log_{10}\alpha\beta$		Experimental value − theoretical value
	Theory	Experiment	
126	11·8	12·7	0·9
247	21·2	26·5	5·3
363	26·9	33·4	6·5

TABLE 3. Values of the constants α and β

6. Conclusions

The experiments reported here seem to lend general support to the theory proposed by Mahony & Smith and questions emerge which warrant further investigation. On a general point, attempts should be made to secure higher accuracy in the curves of marginal stability and water-wave amplitude, for these enable direct quantitative comparisons to be made with the theory. More particularly, it is clear that a detailed investigation of the marginal-stability curves in the region of $\Delta = 0$ is needed, that the possible presence of nonlinearities in the sound field (both in the region of $\Delta = 0$ and elsewhere) should be checked and that the hysteresis of the water-wave amplitude should be explained. Work on these points is in hand.

The authors wish to express their gratitude to Dr J. Ockenden, who first suggested this experiment, and to Dr R. Smith and I. Huntley for the interest they have shown.

REFERENCES

HUNTLEY, I. 1972 Observations on a spatial-resonance phenomenon. *J. Fluid Mech.* **53**, 209–216.

MAHONY, J. J. & SMITH, R. 1972 A model for spatial-resonance phenomena. *J. Fluid Mech.* **53**, 193–207.

PRICE, M. & WILLIAMS, D. C. 1972 Acoustic water-wave interaction. *Final Year Undergraduate Project, Dept. of Engng Sci., University of Oxford*, no. 72–048.